

¹ ebtelplusplus: Efficient Hydrodynamic Modeling of Coronal Loops

³ **W. T. Barnes**  ^{1,2}, **J. W. Reep**  ³, **N. Freij**  ^{4,5}, **S. J. Schonfeld**  ⁶, **R. Collazzo**¹, **P. J. Cargill**^{7,8}, **S. J. Bradshaw**  ⁹, and **J. A. Klimchuk**  ²

⁵ **1** Department of Physics, American University, Washington, D.C. 20016, USA **2** NASA Goddard Space Flight Center, Greenbelt, MD 20771, USA **3** Institute for Astronomy, University of Hawai'i at Manoa, Pukalani, HI 96768, USA **4** SETI Institute, Mountain View, CA 94043, USA **5** Lockheed Martin Solar and Astrophysics Laboratory, Palo Alto, CA 94304, USA **6** Air Force Research Laboratory, Space Vehicles Directorate, Kirtland AFB, NM 87117, USA **7** Space and Atmospheric Physics, The Blackett Laboratory, Imperial College, London SW7 2BW, UK **8** School of Mathematics and Statistics, University of St Andrews, St Andrews KY16 9SS, UK **9** Department of Physics and Astronomy, Rice University, Houston, TX 77005, USA

DOI: [10.xxxxxx/draft](https://doi.org/10.xxxxxx/draft)

Software

- [Review](#) 
- [Repository](#) 
- [Archive](#) 

Editor: 

Submitted: 30 October 2025

Published: unpublished

License

Authors of papers retain copyright and release the work under a Creative Commons Attribution 4.0 International License ([CC BY 4.0](https://creativecommons.org/licenses/by/4.0/))³⁵

¹³ Summary

¹⁴ Understanding the response of the plasma in the solar corona, the outermost layer of the Sun's atmosphere, to heating is of considerable importance in understanding flares and the heating of the quiescent corona. This requires detailed numerical modeling of the coupled system of the coronal plasma and the solar magnetic field¹. While solving the full set of three-dimensional *magnetohydrodynamic* (MHD) equations is feasible for small regions of the corona, the needed computational resources and physical complexity of such models means they are not always amenable to simple or even correct interpretation. Field-aligned hydrodynamic models (e.g. HYDRAD [Bradshaw & Mason, 2003](#)) exploit the fact that the magnetic pressure in the corona is much greater than the gas pressure such that the corona can be considered as a series of mini atmospheres, or *coronal loops*, where the plasma traces out the complex coronal magnetic field. As such, the explicit dependence on the magnetic field can be neglected and the relevant hydrodynamic equations can be reduced to a single-dimension in space: the coordinate along the coronal loop. However, the large range of spatial and temporal scales necessary to resolve this system, in particular the severe time step limitations imposed by thermal conduction, mean that even field-aligned models are computationally expensive enough to make large parameter explorations prohibitive. The enthalpy-based thermal evolution of loops (EBTEL) model ([Cargill et al., 2012; Klimchuk et al., 2008](#)) was originally developed in order to provide a simple and efficient way to study the coronal plasma response to time-dependent plasma heating. EBTEL accomplishes this by computing spatial integrals of the aforementioned field-aligned hydrodynamic equations. The ebtelplusplus software package is a Python and C++ implementation of the EBTEL model and includes effects due to cross-sectional coronal loop expansion, electron-ion coupling, and variable elemental abundances.

³⁶ Statement of Need

³⁷ The key to EBTEL lies in its treatment of enthalpy between the corona and the transition region (TR), the narrow layer of the solar atmosphere that connects the corona with the denser chromosphere below. This enables EBTEL to split the coronal loop into two regions that match across the corona/TR boundary, leading to a set of coupled, non-linear ordinary differential equations that model the spatially-averaged, time-dependent behavior of the relevant

¹This also applies to the coronae of F, G, K, and M dwarf stars.

thermodynamic quantities. EBTEL equates an enthalpy flux with an imbalance between the heat flux out of the corona and the energy lost due to radiation in the TR. If TR radiation cannot balance the downward heat flux, this drives an upflow of material into the corona and if the TR is radiating away more energy than the coronal heat flux can supply this drives a downflow. This approximation is valid for bulk velocities below the local sound speed (Klimchuk et al., 2008).

The EBTEL model was originally developed by Klimchuk et al. (2008). Subsequent improvements to the gravitational stratification and radiative losses by Cargill et al. (2012) gave better agreement with field-aligned hydrodynamic models². Barnes et al. (2016) modified the EBTEL model to relax the single-fluid assumption and treat electrons and ions separately. Cargill et al. (2021) later extended EBTEL to include effects due to cross-sectional area expansion and Reep et al. (2024) added the ability to vary the abundance model for the radiative losses as a function of time. `ebtelplusplus` unifies all of the aforementioned features and solves the following equations for the spatially-averaged electron pressure (p_e), ion pressure (p_i), and number density (n) of a semi-circular coronal loop of half-length L ,

$$\begin{aligned} \frac{1}{\gamma - 1} \frac{dp_e}{dt} &= Q_e + \frac{\psi_c}{L_*} \left(1 + \frac{A_{TR}\psi_{TR}}{A_c\psi_c} \right) - \frac{R_c}{L_*} \left(1 + c_1 \frac{A_{TR}}{A_c} \right), \\ \frac{1}{\gamma - 1} \frac{dp_i}{dt} &= Q_i - \frac{\psi_c}{L_*} \left(1 + \frac{A_{TR}\psi_{TR}}{A_c\psi_c} \right), \\ \frac{dn}{dt} &= -\frac{(\gamma - 1)\xi c_2}{(\xi + 1)\gamma c_3 k_B L_c T_e} \left(\frac{A_{TR} L_c}{A_c L_*} R_c \left(c_1 - \frac{L_{TR}}{L_c} \right) + \frac{A_0}{A_c} (F_{e,0} + F_{i,0}) \right), \end{aligned}$$

where $Q_{e,i}$ are the user-specified heating terms for the electrons and ions, $\psi_{c,TR}$ denote integrals of the electron-ion coupling terms over the TR and corona, respectively, $A_{c,TR,0}$ are the cross-sectional area averaged over the corona and TR and at the TR/corona boundary, respectively, R_c is the energy lost to radiation in the corona, c_1 is the ratio of energy lost to radiation in the TR and corona, $\xi = T_e/T_i$ is the ratio between the electron and ion temperatures, $F_{e,0;i,0}$ are the conductive heat fluxes at the TR/corona boundary for the electrons and ions, $L_{c,TR}$ are the lengths of the corona and TR such that $L = L_c + L_{TR}$, and $L_* = L_c + (A_{TR}/A_c)L_{TR}$. The remaining terms are fixed constants.

This set of equations is closed by an ideal gas law for the electrons and ions: $p_e = k_B n T_e$, $p_i = k_B n T_i$ and $n_e = n_i = n$ due to the assumption of a fully-ionized hydrogen plasma. These equations and their derivations are explained more fully in the aforementioned publications and the `ebtelplusplus` documentation. `ebtelplusplus` solves the above equations using a Runge-Kutta Cash-Karp integration method (see section 16.2 of Press et al., 1992) and an (optional) adaptive time-stepping scheme to ensure the principal physical timescales are resolved at each phase of the loop evolution³. Figure 1 shows example output from `ebtelplusplus` with different model parameters for the same time-dependent heating function.

²This version is sometimes referred to as "EBTEL2".

³The Runge-Kutta Cash-Karp integrator is provided by the [Boost Odeint library](#).

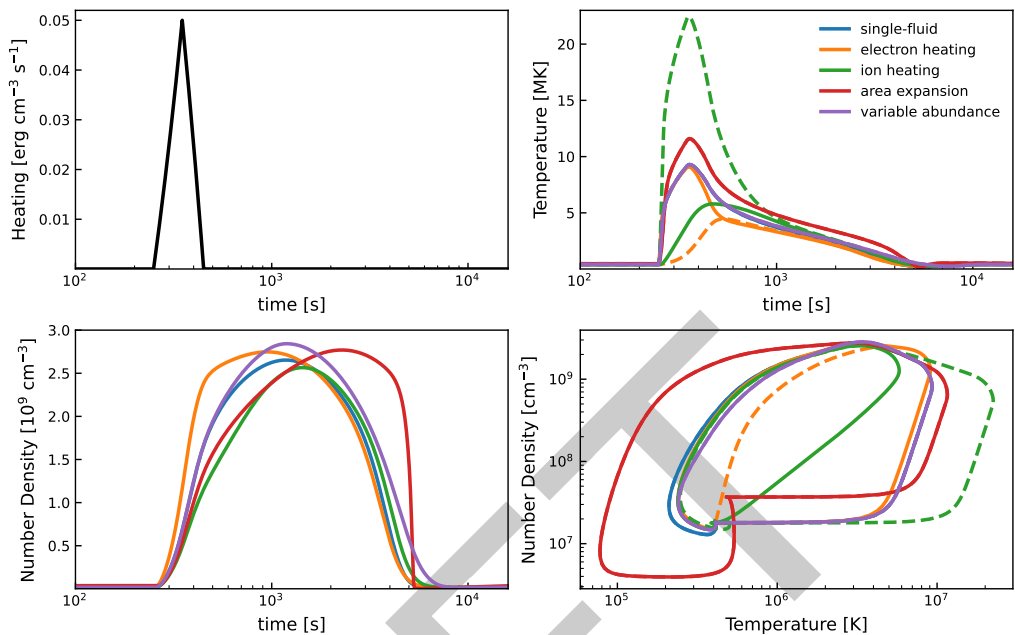


Figure 1: Temperature (top right), density (bottom left), and temperature-density phase space (bottom right) of a coronal loop for five different cases with the same heating input (top left panel). In the nominal case (blue), the electron and ion populations are kept in equilibrium, the cross-sectional area of the loop is constant, and the radiative losses are determined by a power-law function. If the electrons (solid) and ions (dashed) are allowed to evolve separately, heating only the electrons (orange) causes the ions to take about 250 s to fully equilibrate with the electrons while heating only the ions (green) causes the ions to become over three times hotter than the electrons due to the relative inefficiency of ion thermal conduction. Incorporating area expansion through the corona (red) leads to a higher peak temperature and a more delayed peak in the density while calculating the radiative losses using a time-varying abundance (purple) leads to a slightly higher peak density.

73 State of the Field

74 There are currently three separate implementations of the EBTEL model. The original software
 75 implementation of the EBTEL model was in the proprietary Interactive Data Language (IDL).
 76 This implementation, which includes features described in Cargill et al. (2012) and Cargill et al.
 77 (2021), is referred to as **EBTEL-IDL** (Cargill et al., 2024). Comparisons between EBTEL-IDL and
 78 spatially-averaged results from field-aligned hydrodynamic models show very good agreement
 79 (Cargill et al., 2012). Rajhans et al. (2022) relaxed the assumption of subsonic flows in EBTEL
 80 such that the Mach numbers and velocities produced are in better agreement with field-aligned
 81 hydrodynamic simulations for some heating scenarios. The IDL software implementation of
 82 this model is referred to as EBTEL3-IDL. The initial C++ implementation of `ebtelplusplus`
 83 was developed by Barnes et al. (2016) with modifications later made by Reep et al. (2024)
 84 and the Python interface added later. The table below summarizes the features included in
 85 each implementation.

Feature	Citation	EBTEL-IDL	EBTEL3-IDL	<code>ebtelplusplus</code>
Decouple electrons and ions	Barnes et al. (2016)	no	no	yes
Adaptive time step	Barnes et al. (2016)	no	yes	yes
Area expansion	Cargill et al. (2021)	yes	no	yes
Supersonic flows	Rajhans et al. (2022)	no	yes	no

Feature	Citation	EBTEL-IDL	EBTEL3-IDL	ebtelplusplus
Time-variable abundances	Reep et al. (2024)	no	no	yes

86 Software Design

87 The design of the ebtelplusplus software is motivated by two primary needs: 1. computational
 88 efficiency and 2. a high-level, intuitive interface. Both are essential for exploratory analysis of
 89 time-dependent heating of the coronal plasma, including large-scale parameter explorations.
 90 ebtelplusplus is implemented in C++ for computational efficiency and is wrapped in Python
 91 using pybind11 (Jakob et al., 2025) to enable easier installation and a user-friendly API.
 92 As a result, ebtelplusplus is very fast (a single run modeling 10^4 seconds of simulation
 93 time takes only a few milliseconds) and nearly two orders of magnitude faster than
 94 previous IDL implementations. Where appropriate, all inputs and outputs are expressed as
 95 astropy.units.Quantity objects (Astropy Collaboration et al., 2022) to maximize flexibility
 96 and avoid ambiguity. High-level Python objects are provided for configuring additional inputs
 97 and include default values to avoid overly-verbose input configurations.

98 To make the installation process easier for users, precompiled binary wheels for all major
 99 operating systems are distributed via PyPI at every release. This alleviates the need to
 100 compile the C++ code locally and allows new users to start using the software more quickly.
 101 ebtelplusplus is openly-developed on GitHub. Documentation, including an example gallery
 102 and a guide to contributing to the package, is hosted online on Read the Docs.

103 Research Impact Statement

104 Because of its relative simplicity and computational efficiency, EBTEL has been widely used
 105 since its initial development (e.g. Qiu et al., 2012; Ugarte-Urra & Warren, 2014) with Klimchuk
 106 et al. (2008) and Cargill et al. (2012) having nearly 400 citations combined according to
 107 the Astrophysics Data System (ADS). Barnes et al. (2016), which describes the original
 108 implementation of the ebtelplusplus model, has over 50 citations per ADS. In particular,
 109 ebtelplusplus has been used to model thousands of impulsively-heated loops in coronal active
 110 regions (Barnes et al., 2019) and constrain properties of microflares via comparisons with hard
 111 x-ray observations (Marsh et al., 2018).

112 AI Usage Disclosure

113 No generative AI tools were used in the development of this software, the writing of this
 114 manuscript, or the preparation of supporting materials.

115 References

- 116 Astropy Collaboration, Price-Whelan, A. M., Lim, P. L., Earl, N., Starkman, N., Bradley, L.,
 117 Shupe, D. L., Patil, A. A., Corrales, L., Brasseur, C. E., Nöthe, M., Donath, A., Tollerud,
 118 E., Morris, B. M., Ginsburg, A., Vaher, E., Weaver, B. A., Tocknell, J., Jamieson, W., ...
 119 Astropy Project Contributors. (2022). The Astropy Project: Sustaining and Growing a
 120 Community-oriented Open-source Project and the Latest Major Release (v5.0) of the Core
 121 Package. *The Astrophysical Journal*, 935, 167. <https://doi.org/10.3847/1538-4357/ac7c74>
- 122 Barnes, W. T., Bradshaw, S. J., & Viall, N. M. (2019). Understanding Heating in Active
 123 Region Cores through Machine Learning. I. Numerical Modeling and Predicted Observables.
 124 *The Astrophysical Journal*, 880(1), 56. <https://doi.org/10.3847/1538-4357/ab290c>

- 125 Barnes, W. T., Cargill, P. J., & Bradshaw, S. J. (2016). Inference of Heating Properties from
126 "Hot" Non-flaring Plasmas in Active Region Cores. I. Single Nanoflares. *The Astrophysical
127 Journal*, 829, 31. <https://doi.org/10.3847/0004-637X/829/1/31>
- 128 Bradshaw, S. J., & Mason, H. E. (2003). A self-consistent treatment of radiation in coronal loop
129 modelling. *Astronomy and Astrophysics*, 401, 699–709. [https://doi.org/10.1051/0004-6361:20030089](https://doi.org/10.1051/0004-
130 6361:20030089)
- 131 Cargill, P. J., Bradshaw, S. J., & Klimchuk, J. A. (2012). Enthalpy-based Thermal Evolution
132 of Loops. II. Improvements to the Model. *The Astrophysical Journal*, 752, 161. <https://doi.org/10.1088/0004-637X/752/2/161>
- 134 Cargill, P. J., Bradshaw, S. J., Klimchuk, J. A., & Barnes, W. T. (2021). Static and dynamic
135 solar coronal loops with cross-sectional area variations. *Monthly Notices of the Royal
136 Astronomical Society*, stab3163. <https://doi.org/10.1093/mnras/stab3163>
- 137 Cargill, P. J., Bradshaw, S. J., Klimchuk, J. A., & Barnes, W. T. (2024). *Rice-solar-
138 physics/EBTEL: v2.1* (Version v2.1). Zenodo. <https://doi.org/10.5281/zenodo.13351770>
- 139 Jakob, W., Schreiner, H., Rhinelander, J., Grosse-Kunstleve, R. W., Moldovan, D., Smirnov,
140 I., Gokaslan, A., Jadoul, Y., Huebl, A., Staletic, B., Izmailov, S., Cousineau, E., Spicuzza,
141 D., Carlstrom, M., Merry, B., b-pass, Lee, A., Corlay, S., Burns, L. A., ... Šimáček, M.
142 (2025). *Pybind/pybind11: Version 3.0.1* (Version v3.0.1). Zenodo. <https://doi.org/10.5281/zenodo.16929811>
- 144 Klimchuk, J. A., Patsourakos, S., & Cargill, P. J. (2008). Highly Efficient Modeling of Dynamic
145 Coronal Loops. *The Astrophysical Journal*, 682, 1351–1362. <https://doi.org/10.1086/589426>
- 147 Marsh, A. J., Smith, D. M., Glesener, L., Klimchuk, J. A., Bradshaw, S. J., Vievering, J.,
148 Hannah, I. G., Christe, S., Ishikawa, S., & Krucker, S. (2018). Hard X-Ray Constraints
149 on Small-scale Coronal Heating Events. *The Astrophysical Journal*, 864(1), 5. <https://doi.org/10.3847/1538-4357/aad380>
- 151 Press, W. H., Teukolsky, S. A., Vetterling, W. T., & Flannery, B. P. (1992). *Numerical Recipes
152 in C: The Art of Scientific Computing* (Second). Cambridge University Press.
- 153 Qiu, J., Liu, W.-J., & Longcope, D. W. (2012). Heating of Flare Loops with Observationally
154 Constrained Heating Functions. *The Astrophysical Journal*, 752, 124. <https://doi.org/10.1088/0004-637X/752/2/124>
- 156 Rajhans, A., Tripathi, D., Bradshaw, S. J., Kashyap, V. L., & Klimchuk, J. A. (2022). Flows
157 in Enthalpy-based Thermal Evolution of Loops. *The Astrophysical Journal*, 924(1), 13.
158 <https://doi.org/10.3847/1538-4357/ac3009>
- 159 Reep, J. W., Unverferth, J., Barnes, W. T., & Chhabra, S. (2024). Modeling Time-variable
160 Elemental Abundances in Coronal Loop Simulations. *The Astrophysical Journal*, 970, L41.
161 <https://doi.org/10.3847/2041-8213/ad64c3>
- 162 Ugarte-Urra, I., & Warren, H. P. (2014). Determining Heating Timescales in Solar Active
163 Region Cores from AIA/SDO Fe XVIII Images. *The Astrophysical Journal*, 783, 12.
164 <https://doi.org/10.1088/0004-637X/783/1/12>